www.sciencemag.org/content/354/6313/744/suppl/DC1

Supplementary Materials for

Red squirrels in the British Isles are infected with leprosy bacilli

Charlotte Avanzi, Jorge del-Pozo, Andrej Benjak, Karen Stevenson, Victor R. Simpson, Philippe Busso, Joyce McLuckie, Chloé Loiseau, Colin Lawton, Janne Schoening, Darren J. Shaw, Jérémie Piton, Lucio Vera-Cabrera, Jesùs S. Velarde-Felix, Fergal McDermott, Stephen V. Gordon, Stewart T. Cole,* Anna L. Meredith*

*Corresponding author. Email: stewart.cole@epfl.ch (S.T.C.); anna.meredith@ed.ac.uk (A.L.M.)

Published 11 November 2016, *Science* **354**, 744 (2016)
DOI: 10.1126/science.aah3783

This PDF file includes:

Other supplementary material for this manuscript includes the following:

Tables S1 to S14 (Excel format)

TABLE OF CONTENTS

Note 1: Tissue collection and samples analyzed in this study

Anna L. Meredith, Karen Stevenson, Jorge del-Pozo, Darren J. Shaw, Vic R. Simpson, Joyce McLuckie, Stephen V. Gordon, Fergal McDermott, Colin Lawton, Lucio Vera-Cabrera, Jesùs S. Velarde-Felix

The British Isles

A total of 110 dead red squirrels collected between 2004 and 2015 from Scotland (n=44), England (n=26) and Ireland (n=40) were included in this study (Tables S1).

Scottish squirrels were obtained as part of routine scanning surveillance carried out from 2006-2015. Most specimens were roadkill. Out of 508 animals, five had lesions consistent with leprosy, of which three (R13/11, R23/12 and R30/13) were included in this study (Table S1). One additional sample (M406616) was sent by the Scottish Agricultural College of Dumfries, Scotland, with no details on the history of the squirrel (Table S1).

A total of 25 English squirrels from Brownsea Island including eight with leprosy-like lesions (Table S2) were submitted specifically for this study as carcasses. The other English red squirrel arose from a scanning surveillance study during 2002–2012 where three out of 163 animals on the Isle of Wight that showed unusual keratinized or wart-like skin lesions. Histopathology revealed acid-fast bacilli in the pinnae and in one case the spleen. Frozen tissue samples from the most severely affected case (M1960/270411 also called Iow) were therefore included in this study (*31*). Detailed post-mortem examination and collection of tissue samples was conducted either on freshly submitted carcasses, or following freezing and thawing. All carcasses were stored at -20°C. Autopsy results are given in Table S2. Tissue samples (n=214) were obtained from the muzzle, pinna, forelimb and hindlimb, liver, tail, spleen and lung (Table S1), and stored in 70% ethanol and/or 10% neutral buffered formalin. Whole blood or bloody tissue fluid samples were aspirated from the body cavity and stored in plastic tubes at -20°C.

Forty roadkill squirrel carcasses from across Ireland were collected between 2006 and 2012 as part of a project to study the diet of pine martens and stored at -20°C. Only forelimbs were available (Table S1). Four samples from grey squirrels from Penicuik, Scotland were included for PCR and serological screening and TLR1 sequencing (Table S1). Note that, to date, there have been no sightings of grey squirrels presenting with signs of leprosy and postmortem examination of several hundred grey squirrels from Southwest and Northern England, Scotland, and Ireland revealed no lesions suggestive of leprosy.

Observational reports of red squirrels displaying typical lesions consistent with leprosy were submitted to the University of Edinburgh (A.M.) as digital photographs with location information and were mapped as leprosy sightings (Fig. 1)

Mexico

Skin sample PL-02 was obtained from a 49-year-old leprosy patient from Guasave, Sinaloa, Mexico, whose symptoms and histopathology were described previously (*21*).

All tissue samples were shipped to the corresponding research units in 70% ethanol.

Note 2: DNA extraction and confirmation of the presence of leprosy bacilli by PCR

Charlotte Avanzi, Philippe Busso, Karen Stevenson, Joyce McLuckie, Fergal McDermott

All samples from the British Isles and Mexico were screened by PCR for presence of *M. leprae* and *M. lepromatosis.* When possible, screening was done in parallel at two different laboratories (EPFL and Moredun Institute). Details on DNA extraction, PCR screening and screening results are given in Table S3 and Table S4.

Experiments performed at EPFL, Lausanne

Method (1): DNA extraction with host depletion. This method was used to remove host DNA from tissue samples in order to increase the quantity of *M. leprae* or *M. lepromatosis* DNA recovery for whole genome sequencing. DNA was extracted from tissue of 29 red squirrels from the UK and two from Ireland. Tissues (50-200 mg) in 70% ethanol were first rehydrated in Hank's balanced solution (Thermo Fisher Scientific, USA, MA) prior to mincing with scissors. Cells were detached from the tissue by 30 min incubation at 37°C with a mixture of 0.5 U of collagenase and dispase (Roche Diagnostics, Mannheim, Germany) for skin tissues or 0.13 U of liberase (Roche Diagnostics, Mannheim, Germany) for internal organs, followed by incubation at 56°C with 10 mg/ml of trypsin (Sigma-Aldrich, St. Louis, Missouri, USA) until complete digestion. Free cells were then resuspended in 1 mL of phosphate-buffered saline (PBS) and DNA was extracted using the QIAmp DNA microbiome extraction kit (Qiagen, Hilden, Germany) according to the manufacturer's recommendations. Briefly, human cells were first lysed and host nucleic acids were digested with a benzonase nuclease. Bacterial cells were then lysed using chemical and mechanical disruption, followed by DNA precipitation and purification on silica column. Each run of extraction included a batch of 5 to 9 samples and one blank control (500 µl of Hank's balanced solution).

Total DNA extraction. Total DNA extraction without host depletion was used for PCR screening of red (n=80) and grey (n=4) squirrel samples from Scotland and Ireland (Table S3). In addition, red squirrel samples from Scotland (n=3) and England (n=26) were re-extracted to sequence the *TLR1* gene, encoding toll like receptor 1, as well as the four grey squirrels from Scotland. Approximately 50-200 mg of tissue were collected and rehydrated in Hank's balanced solution prior to mincing with scissors. Total DNA was then extracted using the QIAmp UCP pathogen Mini Kit (Qiagen Hilden, Germany) but with a modified protocol. Tissue was digested for 2 h at 56°C with 500 µl of lysis buffer (buffer T) and a mixture of proteinase K (20 µl, 20 mg/ml) and lysozyme (20 µl, 10 mg/ml). An additional mechanical disruption step, using zirconia beads, was used to increase the lysis of mycobacterial cells. The supernatant recovered from the digestion step was mixed in a bead-beating tube containing 500 µl of zirconia beads 0.1 mm and placed in a bead-beater instrument, and a velocity of 6.5 m/s applied twice for 45 s with a 5 min interval, while samples were stored on ice. Then, an additional step of 30 min at 56°C with proteinase K (20 µl, 20 mg/ml) and lysozyme (20ul, 10 mg/ml) was applied followed by treatment with APLc buffer for 10 min at 70°C. DNA was precipitated and purified on QIAamp UCP Pathogen Mini silica column then quantified using the Qubit dsDNA HS Assay Kit

with the Qubit 2.0 Fluorometer (Life Technologies). Each extraction run included a batch of 5 to 9 samples and one extraction blank (500 µl of Hank's balanced solution).

PCR amplification. PCR amplification was performed using specific primer pairs LPM244 (*11*), which amplify a 244-bp fragment from the *hemN* gene of *M. lepromatosis*, and RLEP 7 and 8 (*23*), which amplify a 500 bp fragment of the RLEP repetitive sequences in *M. leprae*. An additional primer set targeting the mitochondrial 12S ribosomal RNA gene of the red squirrel (GenBank: D50287.1) was used to assess the performance of DNA extraction methods and in blank samples. Primers were designed using Primer3 web-tool (http://primer3.sourceforge.net) and are listed in Table S14. PCR amplifications were performed in a 50 µL reaction volume containing AccuStart II GelTrack SuperMix (Quanta BioSciences, Gaithersburg, MD), 4 µL of each primer at 2 µM, and 2 µL of DNA extract or sterile distilled water for post-mortem specimens, positive controls (DNA from *M. lepromatosis* strain Mx1-22A (*11*) and *M. leprae* strain Thai-53 (*23*)), and negative controls.

Amplification started with an initial denaturation step of 3 min at 95°C, followed by 40 cycles of 30 s denaturation at 95°C, 40 s primer annealing at 58°C, and 30 s extension at 72°C, followed by a 10 min final extension at 72°C. The amplicons obtained were then analyzed by electrophoresis on a 1% agarose gel, stained using GelRed (Chemie Brunschwig, Basel, Switzerland) and visualized on a UV transilluminator. Where sequence confirmation was required, the PCR products were subjected to enzymatic treatment with Illustra ExoProStar 1-Step (GE Healthcare Life Sciences) and sequenced using a BigDye Terminator version 3.1 Cycle Sequencing kit and analyzed on a ABI3130 XL DNA sequencer (Applied Biosystems, ThermoFisher, FC, California, USA). Sequences were aligned against the corresponding reference sequences using CodonCode aligner software (version 5.0.1; CodonCode Corporation, Dedham, MA).

Experiments performed at the Moredun Research Institute, Scotland

Joyce McLuckie, Karen Stevenson

DNA was extracted using a Qiagen DNeasy Blood and Tissue kit on samples from 48 red squirrels (n=48) from Scotland and England (Table S3). Briefly, a small piece of tissue (10-15 mg) was excised using a sterile scalpel blade and then lyzed using 0.1 mm silica beads (Lysing Matrix B, MP Biomedicals) in 320 µl ATL tissue lysing buffer (Qiagen DNeasy Blood and Tissue Kit) in a FastPrep™ FP120 (Thermo Savant) for three cycles of 20 s at 6m/s with cooling on ice in between. Beads and debris were pelleted in a microfuge and the supernatant transferred to a fresh microcentrifuge tube. Proteinase K (20 µl, Qiagen DNeasy Blood and Tissue Kit) was added and the sample incubated overnight at 56°C. DNA was extracted using the spin column protocol according to Qiagen DNeasy Blood and Tissue Kit instructions. For each batch of DNA extractions, two extraction controls were included; sterile distilled water (50 µl) and a sample of tissue known to be free from the target organism. Extracted DNA was quantified using a NanoDrop® ND-1000 (Thermo Scientific).

PCR amplification was performed using the specific primer pairs LPM244 (*11*) and RLEP 7 and 8 (*23*) as described above. PCR amplifications were performed in a 50-µl reaction volume containing GoTaq Flexi buffer (Promega) (MRI), 4 µl of each primer at 2 µM, and 2 µl of DNA extracts or sterile distilled water for post-

mortem specimens, positive controls (*M. lepromatosis* strain Mx1-22A (*11*) and *M. leprae* strain Thai-53 (*23*)), and negative controls. The amplification started with an initial denaturation step at 95°C followed by 40 cycles of 30 s denaturation at 95°C, 40 s primer annealing at 58°C, and 30 s extension at 72°C, followed by a 10-min final extension at 72°C. The amplicons obtained were then analyzed by electrophoresis on a 1% agarose gel, stained using GelRed (Chemie Brunschwig, Basel, Switzerland) and visualized by using a UV transilluminator. Where sequence confirmation was required, the PCR products were sent to MWG BioTech for amplicon sequencing.

Results

A total of 172 tissue samples (TS) from the 114 squirrels were screened by PCR for the presence of *M. leprae* and/or *M. lepromatosis* at EPFL and/or the Moredun Institute using different DNA extraction methods (Table S3 and S6). For each squirrel we screened one to five TS mainly from the muzzle, pinna, hindlimb or footpad and tail but occasionally PCR was performed on organs such as the liver, spleen or lung. We considered a specimen infected if at least one of the TS was PCR-positive.

M. lepromatosis

M. lepromatosis was detected by PCR in all four squirrels with leprosy-like lesions from Scotland and from the Isle of Wight (n=1). For two of these specimens, (R13/11 and R30/13), different tissues were screened by PCR and all showed *M. lepromatosis* positivity. *M. lepromatosis* was also detected in two specimens from 40 red squirrels with no macroscopic lesions from Scotland (2/40 or 5% of cases) and in two out of 40 red squirrels with no macroscopic lesions from Ireland (2/40: 5% of cases). *M. lepromatosis* was not detected in samples from Brownsea Island (n=25) nor in grey squirrels from Scotland (n=4)

M. leprae

M. leprae was found in all 25 specimens from Brownsea Island but was not identified in any samples from Scotland (n=44) or Ireland (n=40). Some differences in PCR positivity were found between tissues from four specimens from Brownsea Island (Brw15-3, Brw15-5, Brw15-11, Brw15-22) due to the use of different muzzle and pinna samples by different laboratories.

Note 3: Serology

Karen Stevenson, Joyce McLuckie, Lucio Vera-Cabrera, Jesùs S. Velarde-Felix

Blood samples were tested for *M. leprae*- and *M. lepromatosis*-specific antibodies using a chromatographic immunoassay developed for use with human blood samples: the ML Flow test developed by KIT (Royal Tropical Institute) Biomedical Research in Amsterdam with the financial support of the Netherlands Leprosy Relief. For the squirrel samples, either whole blood or sera were tested following the instructions provided by the test manufacturers. Test results were interpreted both at 5 and 10 min. For each batch of samples, a positive control serum (human serum P13LL from a leprosy patient) and a negative control serum (R1695 from a red squirrel showing no clinical signs) was used. Results are shown in Table S4 and they are scored from 0 to 2, with 0 for a negative result, 1 for a weak result (positivity after 5 min of incubation) and 2 for a strong result (positivity before 5 min of incubation). Serology was performed on 27 samples from Scotland (n=1) and England (n=22) (Table S1 and S4). Among the four grey squirrels screened by serology, none of them showed positivity.

For the human sample, PL-02, from a Mexican patient presenting with diffuse lepromatous leprosy (DLL), as well as the unique red squirrel screened from Scotland, the ML flow test was also used and showed a positive result after 5 min indicating that this test can be used to detect *M. lepromatosis* infections as predicted by genome analysis (*11*).

Blood/sera were available for 22 red squirrel specimens from Brownsea Island of which 6 showed strong positivity, 6 were weakly positive whereas 10 were negative. Among the 14 samples from asymptomatic animals, 3 were high strong positives, 5 were weak and 6 were negative. Among the 8 specimens from diseased animals with gross lesions and RJ classification, 4 were positive and 4 were negative. The lowest BI (from 0 to 2) was observed for Brw15-12 but this animal was highly positive for PGL-1 antibodies. On the other hand, Brw15-6 showed a bacillary index from 1 to 3 and was negative by serology.

Thus, these results showed that there is no correlation between the disease severity, RJ classification and BI with the anti-PGL-1 titer in blood. This difference compared to human data (*17*, *18*) might be due to weak affinity of the secondary anti-human IgM antibody. Further analyses using rodent secondary antibodies are needed.

Note 4: Histopathology

Histopathology was carried out on 29 specimens from Scotland and England (Table S1) as well as on 5 specimens from Ireland

Experiments performed at the University of Edinburgh, Scotland

Jorge Del-Pozo, Anna L. Meredith

A gross post-mortem examination was conducted on all PCR-positive squirrels from Scotland and Brownsea Island. This was followed by collection of skin samples from the muzzle, eyelids, pinna, forelimb, hindlimb, as well as spleen and liver samples. These samples were fixed for a minimum of 24 h in 10% neutral buffered formalin (NBF) and processed for histology in an Excelsior Electron tissue processor (Thermo Scientific, UK). This involved replacement of the water in the sample with paraffin by serial exposure to: 70% ethanol (1 h), 90% ethanol (1 h), absolute ethanol (4 x 1 h), xylene (2 x 1 h), and paraffin (3 x 1.3 h). All the tissues were then sectioned at 4 μm thickness and stained with *haematoxylin-and-eosin* (H&E) and Ziehl Neelsen (ZN) stains. All slides were examined by a board-registered veterinary pathologist and their histological features recorded. The features of granulomatous dermatitis were further documented by establishment of Ridley-Jopling (RJ) classification (*32*) bacterial index (BI), granuloma severity/distribution, presence/absence of neuritis and intraneural acid fast bacilli (AFBs).

Results

Gross pathology (Table S2)
When present, just like the features of wild sightings of affected squirrels, the gross pathological presentation at post-mortem examination was similar for both squirrels positive for *M. lepromatosis* (n=4) or for *M. leprae* (n=8). The main feature of this presentation is the presence of moderate to severe areas of cutaneous swelling and alopecia. The areas involved were the muzzle and both pinna in all the squirrels, with variable bilateral involvement of the eyelid (67% *M. lepromatosis* and 38% *M. leprae*), ventral aspect of the tarsal area (100% and 88%), and carpal area (0% and 13%), and urogenital area (0% and 38%). Ulceration of these lesions was only noted in four squirrels of both groups that featured superimposed secondary bacterial infection in histology (not pictured). Our sample set includes 17 squirrels that did not present with gross pathological changes but were PCR-positive for *M. leprae*.

Histopathology (Table S5)
All *M. lepromatosis* PCR-positive squirrels (n=4) had gross lesions. In these, the histological presentation of cutaneous lesions was frequently consistent with severe lepromatous leprosy (LL) in the RJ scale (LL, 75% of cases), with diffuse sheets of foamy macrophages (Virchow cells), sparse lymphocytes, and a BI ranging from 3+ to 5+ (Fig S1). Severity and BI were anatomic location dependent, with generally lower BI and severity in hindlimb lesions when compared with facial lesions. The histological presentation featured neuritis (perineural or intraneural) with intraneural and intravascular AFB in all cases. Less frequently, the presentation was consistent with moderate borderline lepromatous leprosy (BL, 25%), with a multifocal,

frequently perineural presentation featuring numerous lymphocytes and plasma cells and a BI of 3+. There was perineural neuritis with no intraneural or intravascular AFB in the BL case. With regards to systemic spread, there was no involvement of thoracic or abdominal organs in any case, and there was retropharyngeal lymphadenitis with intra-lesional AFBs in one LL squirrel.

In *M. leprae* PCR-positive squirrels with gross leprosy lesions (n=8), 75% presented with LL lesions with diffuse sheets of Virchow cells and a BI ranging from 2+ to 3+. Lesions consistent with BL were noted in the remaining 25%, with a BI ranging from 1+/2+. Sharply defined neuritis with intraneural AFB was noted in all cases, which was always perineural, and occasionally also intraneural (25%). Systemic involvement, featuring granulomatous splenitis with intralesional AFB was seen in 37.5% cases. There was also anatomical location-dependent variation in lesion severity with lower BI and severity in hindlimb lesions. Location had an influence on the RJ classification in two cases (i.e. BL in the muzzle of an otherwise LL squirrel, and BT in the pinna of of an otherwise BL squirrel – Fig S2). Intravascular AFBs were absent.

The remainder of the *M. leprae* PCR-positive squirrels is composed of animals devoid of gross leprosy lesions (n=17). Leprosy-associated histological lesions were absent in 64.7% of these squirrels. In the remaining 35.3% the presentation exclusively featured mild chronic perineuritis of the pinna and/or muzzle. Intraneural AFB were only noted in superficial submucosal nerves at the cranial-most aspect of the nasal cavity of one of these squirrels.

In both *M. lepromatosis* and *M. leprae* PCR-positive squirrels with gross leprosy lesions, 58.3% of the animals had an ulcerative component to the cutaneous lesion in one or more of the locations involved (frequently in facial lesions). This was invariably associated with the presence of a second bacterial population in the lesion at that location. In all but one of these cases, the second bacterium was filamentous and Gram-positive, forming extracellular dermal colonies. In the remaining case, the bacteria were Gram-positive cocci forming colonies at the surface of the ulcerated lesion. These bacteria were interpreted as secondary invaders of the lepromatous lesions and vasculitis was not noted in any of these cases.

Experiments performed at University College Dublin, Ireland

Janne Schoening

To examine for evidence of *M. lepromatosis* infection, both forelimbs were removed. Sections of the left or right footpad were used for DNA extraction at EPFL with downstream PCR-screening and genome sequencing as described above. The contralateral limb of both PCR-positive squirrels (Ir25 and Ir36) and three PCR-negative squirrels (Ir03, Ir30 and Ir38) was processed at UCD for histopathological examination using standard procedures. Immediately after thawing, sections of the footpad and dorsum of the foot were fixed in 10% neutral buffered formalin and embedded in paraffin. Four-micron-thick sections were routinely stained with H&E, as well as ZN staining, and examined using a Nikon Eclipse E600 microscope.

Results

After examination of the footpad and dorsum of the foot sections, no AFB were present in Ir03, Ir30, Ir38 and Ir25. However, several AFB were found in both regions for Ir36 (Fig. S3). In addition, in the adjacent subcutis were scattered mononuclear cells, presumably macrophages, containing single to numerous intra-cytoplasmic AFB. Also present in this area was a focal infiltration with moderate numbers of mononuclear cells (presumably plasma cells with scattered macrophages) of unclear significance that was not associated to the AFB-containing cells. Further scattered intra- and extracellular AFB were present throughout the subcutis of the footpad. Several cross-sections of peripheral nerve were present within the section but not affected. There were no granulomas present.

Experiments performed at Veterinary Investigation Center, England

Vic R. Simpson

Macroscopic and microscopic lesions were analyzed as described in (*18*) and (*31*).

Results

The gross pathology in the Isle of Wight case with *M. lepromatosis* did not closely resemble the Scottish cases but showed crusty thickening of the pinnae with keratinised or wart-like protuberances, clearly circumscribed wart-like growths on the bridge of the nose and on one flank, most digits and the tail tip. Histopathological lesions included marked epidermal papilliform hyperplasia, orthokeratotic hyperkeratosis and a variable dermal inflammatory cell infiltration. Sparse numbers of AFB were observed in bands of macrophages aligned closely to the cartilage of the pinna. AFB were also present in the spleen (*18*).

Note 5: Genome-wide sequencing

Charlotte Avanzi, Philippe Busso, Andrej Benjak

After confirmation of the presence of the bacilli by PCR, whole-genome sequencing was performed on 43 DNA extracts (Tables S1 and S3).

5.1 Library preparation

DNA samples were sonicated to obtain 500 bp long fragments with the S220 Covaris (Covaris) using the manufacturer's protocol. 50 µl of each extract were used for indexed library preparation following the protocols described below and 2 µl were used for quantification using the Qubit dsDNA HS Assay Kit and the Qubit 2.0 Fluorometer (Thermo Fisher Sc., USA, MA). Sequencing libraries were synthesized with the Kapa Hyper prep kit (Kapa Biosystems, Wilmington, MA, USA), according to the manufacturer's instructions. PentAdaptersTM (PentaBase, APS, Denmark) were used to barcode the library and were diluted according to Kapa's recommendation and the starting DNA concentration. After the final amplification step, libraries were then quantified using Qubit dsDNA BR Assay Kit (Thermo Fisher Sc., USA, MA) and the fragment size was assessed on a Fragment Analyzer (Advanced Analytical Technologies, Inc. Ankeny, USA). Finally, libraries were multiplexed (1/30) and sequenced using single-end reads on an Illumina HiSEq 2500 instrument or as paired-end reads on a MiSeq instrument.

5.2 Array design for *M. lepromatosis* sequence capture

Probes for an Agilent 1-million feature array were designed using PanArray v1.0. (*33*). Both forward and reverse-complement sequences of the *M. lepromatosis* Mx1-22A genome sequence were used (*11*). Probe length was 60 nucleotides, and the tiling window size was set to 7.

5.3 Enrichment and sequencing of genome-wide enriched samples

Samples Ir27 and Ir36, which were PCR positive for *M. lepromatosi*s, were extracted 6- and 4-times respectively from 50-100 mg of tissue each using the DNA extraction method with host depletion, described above in section (Note 2). Library preparation was according to the protocol described above. The 10 amplified libraries were pooled in equimolar amounts (around 1.5 µg of amplified library) and captured on an array as described above (*3*). After hybridization, the captured products were eluted in 490 µl of water, quantified by Qubit and amplified for 10 cycles in 100 µl reactions containing 40 µl of template, 50 µl of 2X Kapa HiFi HotStart Ready Mix and 10 µl of primer mix (Kapa Biosystems, Wilmington, MA, USA). The following thermal profile was used: a 45 s initial denaturation at 98°C, 10 cycles consisting of 15 s denaturation at 98°C, a 30 s annealing at 60°C and a 30 s elongation at 72°C, followed by a 1 min final elongation at 72°C. The amplified library pool was purified, its concentration was determined using Qubit technology and the fragment size distribution was evaluated using a Fragment analyser. Sequencing was carried out on an Illumina HiSeq platform using the manufacturer's protocol for multiplexed sequencing (HiSeq SR Cluster Kit v4 cBot).

5.4 Availability of sequence data

Illumina reads were deposited at Sequence Read Archive (SRA) database under accession numbers SRR3672737 to SRR3672758 (SRA Study SRP076631, NCBI BioProject PRJNA325727), and SRR3673933.

Note 6: Genome-wide analysis

Andrej Benjak, Chloé Loiseau

6.1 Processing of reads

Raw data for previously published samples were retrieved from public repositories (*11*). For all Illumina datasets, reads were adapter- and quality-trimmed (average base quality at least 15 over a 5-base sliding window) with Trimmomatic v0.33 (*34*). Reads shorter than 40 bases were discarded. Overlapping paired-end reads were merged with SeqPrep (https://github.com/jstjohn/SeqPrep).

6.2 Mapping

Mapping was done with Bowtie2 v.2.2.5 (*35*) using default parameters. Duplicate reads were marked with the MarkDuplicates module from Picard v1.139 (https://github.com/broadinstitute/picard). Reads with a mapping quality below 8 (unspecific mapping) were discarded. For *M. leprae*, strain TN (GenBank accession number AL450380.1) was used as reference, while for *M. lepromatosis*, strain Mx1-22A (GenBank accession number JRPY00000000.1) was used.

Alignment of *M. leprae* finished genome sequences (Br4923 and Kyoto-2) against the *M. leprae* TN reference was done with LAST (*36*) using default parameters. For alignment of finished genome sequences between *M. leprae* and *M. lepromatosis* LAST was used with the gamma-centroid option. To efficiently align *M. lepromatosis* short reads with the *M. leprae* reference (used for calculating the Neighbor-Joining phylogenetic tree) a consensus sequence was inferred from the alignment of *M. lepromatosis* and *M. leprae* reference sequences, omitting InDels (Insertions and deletions). In other words, *M. lepromatosis* SNPs were transferred onto the *M. leprae* reference sequence. This facilitated Bowtie2 mapping of otherwise diverged sequences (average 12% nucleotide diversity between *M. leprae* and *M. lepromatosis*) without sacrificing stringency.

6.3 Variant calling

Variants were called with VarScan v.2.3.7 (*37*) with the following thresholds: minimum overall coverage of 5 reads, minimum variant support of 3 reads, minimum average base quality of 15, minimum variant frequency of 20%, minimum frequency for a homozygous variant of 80% and maximum frequency of reads on one strand of 90%. Heterozygous sites (20-80% SNP frequency) were omitted. For *M. leprae*, regions corresponding to rRNA genes, repeats and positions identified in the negative control sample SK12 (*3*) were omitted. For *M. lepromatosis*, sites with consensus bases in the reference sequence were omitted. Variants and multiple alignments were manually checked for possible errors or inconsistencies. Suspicious sites were omitted.

6.4 Phylogeny

Phylogeny was done on SNP alignments using MEGA6 (*38*). For Maximum Parsimony (MP), separate SNP alignments for either *M. leprae* samples or *M. lepromatosis* samples were used to maximize the number of informative sites in each group. SNP alignment of *M. leprae* contained a total of 873 variable sites, while that of *M. lepromatosis* contained 436 variable sites. For each alignment, the sequence of the outgroup (*M. lepromatosis* for *M. leprae* and *vice versa*) was retrieved corresponding to the variable sites within each group. To calculate MP trees, all

positions with <90% site coverage were eliminated i.e. <10% alignment gaps and missing data were allowed at any position. This resulted in 671 sites used for *M. leprae* and 435 sites used for *M. lepromatosis*. The MP trees were obtained using the Subtree-Pruning-Regrafting (SPR) algorithm with search level 1 in which the initial trees were obtained by the random addition of sequences (10 replicates). Branch lengths were calculated using the average pathway method and units are the number of changes over the whole sequence. Bootstrap testing was done on 500 replicates.

For Neighbor-Joining, a single SNP alignment of all samples was used, consisting of 311,324 sites. All positions with <90% site coverage were eliminated i.e. <10% alignment gaps and missing data were allowed at any position. This resulted in 307,159 sites used for calculation of the tree. The evolutionary distances were computed using the p-distance method (*39*) and units are the number of base differences per site. Bootstrap testing was again done on 500 replicates.

6.5 Dating analysis

Dating analysis was done using BEAST v1.8.2 (*24*). Separate SNP alignments for either *M. leprae* or *M. lepromatosis* samples were used to maximize the number of informative sites in each group. For *M. leprae*, sample S15 was removed from the analysis because it contains an unusually high number of SNPs (*3*), probably related to its drug resistance including to rifampicin and dapsone. Also, four samples from three specimens from Brownsea Island were omitted because there were too many gaps in the alignments. Sites with gaps or missing data were removed, resulting in 498 variable sites for *M. leprae* and 432 variable sites for *M. lepromatosis*. For the analysis of *M. leprae* strains, the calibrated radiocarbon dates for the five ancient genomes as well as the isolation years for the modern genomes were used as priors (*3*). The strict-clock model with uniform rate across branches, with general time reversible (GTR) substitution model and constant population size was used for the analysis. One Markov chain Monte Carlo (MCMC) run was carried out with 50,000,000 iterations, sampling every 2,000 steps. The first 1,000,000 iterations were discarded as burn-in. A substitution rate of 6.87 $x10^{-9}$ substitutions per site per year (4.62-9.12 $x10^{-9}$ 95% highest posterior density, HPD) was estimated, which is close, and in between the substitution rates estimated in (*3*) on a similar dataset (6.13 $x10^{-9}$; 3.38-8.56 $x10^{-9}$ 95% HPD) and in (*11*) (7.67 $x10^{-9}$; 1.11 x^{-8}-4.2 $x10^{-9}$ 95% HPD) where *M. lepromatosis* was used together with *M. leprae* strains.

The substitution rate calculated here for *M. leprae* was applied in the analysis of *M. lepromatosis* strains. Strict-clock model with normal rate across branches, with Hasegawa, Kishino and Yano (HKY) substitution model and constant population size was used for the analysis. One MCMC run was carried out with 50,000,000 iterations, sampling every 2000 steps. The first 1,000,000 iterations were discarded as burn-in. Applying the substitution rates reported in (*3*) and (*11*) gave similar results, as expected.

Results of dating analysis

For *M. leprae* strains (excluding those mentioned above), we estimated a substitution rate of 6.87 x10-9 substitutions per site per year (4.62-9.12 x10-9 95% HPD), which is very close to the previous estimation on a smaller dataset (6.13 x10-9; 3.38-8.56 x10-9 95% HPD). The resulting diverge time for the MRCA of all *M. leprae* strains was 3,483 ya, which is similar to the previously estimated 3,126 ya in (*3*).

Applying the same substitution rate estimated for *M. leprae* to analyse the *M. lepromatosis* strains, we estimated the divergence time for the MRCA of all *M.*

lepromatosis strains to be 26,869 ya. Divergence time for the two Mexican strains was 186 ya and that for all European strains was 379 ya.

Results of the genome-wide analysis

We have sequenced 44 genomes (Table S7) including 19 with more than 5X coverage of *M. leprae* (n= 9) and *M. lepromatosis* (n=12) genomes. We analyzed cases where more than one dataset (from different biopsies) was available for the same animal, and we determined that there was no variation within the same animal, so for phylogenetic and dating analysis we chose one dataset with the best read coverage (in bold, Table S7), or as for the sample from the Isle of Wight and sample Brw-15 from Brownsea island, we merged the datasets from two biopsies to increase the overall read coverage.

- **SNP analysis *M. lepromatosis* strains.**

We determined the pairwise SNP differences between *M. lepromatosis* strains (Table S8). Only seven SNPs differentiate between the two human strains from Mexico. Three of these SNPs were in intergenic regions, two were in pseudogenes and two were missense mutations in genes *adhA* (MLPM_2053, 28A>G) and *atpB* (MLPM_1139, 341G>A).

There are no more than 11 SNP differences between all strains from squirrels.

However, there are around 400 SNPs between the Mexican and British strains. Among them, 117 are in intergenic regions, 89 are non-synonymous and 79 are synonymous substitutions in coding genes, 151 are in pseudogenes. Thus, the *M. lepromatosis* strains from Mexico and those from the British Isles belong to distinct lineages (**Figs S4 and S5**).

- **SNP and phylogenetic analysis of *M. leprae* strains.**

We found virtually no genetic variation between the Brownsea Island strains (only three SNPs), which is not surprising given the elevated population density of red squirrels, the isolation and the small area of the island. Overall, 37 SNPs and 3 InDels distinguish Brownsea Island strains from other strains in this study Table S9.

The *M. leprae* strain from the Brownsea Island belongs to SNP subtype 3I as previously described in human medieval samples from England and Denmark (*3*), and from the Americas (*23*). In addition, the strain belongs to the same SNP subtype as the one reported in wild armadillos in the USA where zoonosis and anthroponosis are likely occurring (*9*). Phylogenetic relationship between ancient, modern, and animal SNP type 3I shows that Brownsea Island strains form an independent clade, which branches between human medieval *M. leprae* strains Jorgen_625 and SK2 (Fig S1 and S2). So the strain that currently infects red squirrels from Brownsea Island may be derived from a human strain, which was circulating in medieval Europe.

SNP type 3I is the only genotype associated to date with infections in humans and wild animals. We first compared the genomes of animal strains to those of other SNP subtype 3I strains but found no specific SNP to be associated with animal species. Then, we compared all polymorphisms (SNPs, InDels) to those in other *M. leprae* genotypes (see Table S10).

Note 7: Identification of mutations in *TLR1* of *Sciurus vulgaris* and structural modeling of TLR1

Charlotte Avanzi, Andrej Benjak, Philippe Busso, Jérémie Piton, Stewart T. Cole

7.1 Determination of the *TLR1* consensus sequence

Neither *TLR1* sequences of *Sciurius vulgaris* nor *S. carolinensis* were publicly available. In order to obtain a preliminary consensus sequence of *TLR1* we iteratively mapped our short-read datasets from red squirrels against the *TLR1* region from the publicly available genomic sequence of the thirteen-lined ground squirrel (*Ictidomys tridecemlineatus*) using BBMap (https://sourceforge.net/projects/bbmap/), Bowtie2 (*35*) and manual curation. This enabled us to design seven sets of primers spanning the entire *TLR1* coding sequence to fill gaps in the draft consensus sequence. PCR amplifications were performed as described above (2.2) with the AccuStart II GelTrack SuperMix kit. PCR was performed on 81 samples extracted with the method (*2*) (Table S11).

7.2 Long range PCR and sequencing

TLR1 shows a high level of nucleotide similarity with *TLR6* especially in the TIR domain region (*40*). Therefore, using primers in the coding sequence of *TLR1* could lead to unspecific amplification. In order to obtain the complete sequence of *TLR1*, we designed primers flanking the TLR1 coding exon (Table S14**)** and amplified 2.7 kb-long amplicons.

PCR amplifications were performed in a 50-µl reaction volume containing 25 µl of Phusion HF buffer (Thermo Fisher scientific, USA, MA), 4 µl of each primer at 2 µM, 1 µl of dNTPs at 10mM; 0.2 µl of Phusion polymerase and 5 µl of DNA extracts or sterile distilled water for post-mortem specimens, and negative controls. The amplification started with an initial denaturation step for 30 s at 98°C followed by 35 cycles of 10 s denaturation at 98°C, 30 s primer annealing at 65°C, and 3 min extension at 72°C, followed by a 10 min final extension at 72°C. Amplicons were electrophoresed on a 1% agarose gel, stained using GelRed (Chemie Brunschwig, Basel, Switzerland) and visualized on a UV transilluminator. PCR products were subjected to enzymatic treatment with Illustra ExoProStar 1-Step (GE Healthcare Life Sciences) prior to library preparation.

Long range PCR was performed on 81 samples and the 58 samples that produced good amplicons were selected for sequencing (Table S12). Fragmentation was performed by an enzymatic procedure. Briefly, 32 µl of amplicons were mixed with 4 µl of 10X Fragmentase Reaction Buffer v2 (New England Biolabs, USA, MA) and 4 µl of ds Fragmentase. The mix is incubated 5 min at 37°C and the reaction stopped with 10 µl of EDTA 0.5M. The reaction was purified using AMPure XP beads (Beckman Coulter USA, IN) with a 1.8X volume. Illumina libraries were prepared as described above (*11*). All samples were sequenced together on an Illumina MiSeq using the manufacturer's protocols for multiplex sequencing (MiSeq Reagent kit v3 600 cycles).

7.3 *TLR1* analysis

Illumina reads were adapter- and quality-trimmed (average base quality at least 15 over a 5-base sliding window) with Trimmomatic v0.33 (*34*). Reads shorter than 40 bases were discarded. Overlapping paired-end reads were merged with SeqPrep

(https://github.com/jstjohn/SeqPrep). Reads were mapped against the draft TLR1 sequence described above and processed with VarScan v.2.3.7 (*37*). Minimum variation frequency was set at 10%, and minimum frequency for a homozygous call was at 90%.

Odds ratio (OR), standard error and 95% confidence interval were calculated according to Altman, 1991 (*41*).

7.4 TLR1 structural modeling

Red squirrel TLR-1 was modeled by using in combination two homology modeling web servers, PHYRE2 (*42*) and SWISS-MODEL (*43*). The N-terminal extracytoplasmic part (residue 30-573) was modeled using the human TLR-1 crystal structure as template (PDB code: 2Z7X, (*44*)) and the intracellular C-terminal part (628-788) using the crystal structure of the Human TLR-1 TIR domain (PDB code: 1FYV, (*45*). The linker and membrane part of the Red squirrel TLR-1 (589-627) were built using the Homology Model fitted in the Electron Microscopy map of the full-length human TLR-5 as template (PDB code: 3J0A, (*46*)). Orientation and position of the two domains were deduced from previous studies (*47*) and the identification of the membrane part was done with the help of THMM web server (*48*). Illustrations were made using Pymol software (*49*).

7.5 Availability of sequence data

Illumina reads from *TLR1* were deposited at Sequence Read Archive (SRA) database under accession numbers SRR3674396 to SRR3674450 (NCBI BioProject PRJNA325827) and accession numbers SRR3674451 to SRR3674453 (NCBI BioProject PRJNA325856).

Representative TLR1 sequences of red and grey squirrels were deposited at GenBank under accession numbers KX388139, KX388140 and KX388141. These derive from samples Brw15-12, Ir15 and G12562 respectively.

Results

Two polymorphisms have been described for human *TLR1*. One in the cytoplasmic region of the receptor involves the modification of an isoleucine to a serine at position 602 (I602S, T1805G) and this impairs the trafficking of the receptor to the cell membrane but confers resistance to disease (*40*). The other variant is found in the external ligand-binding site of the receptor and involves the modification of position 248 (A743G) where the presence of asparagine decreases the activity of TLR1. Like I602S, the 248S genotype is associated with leprosy whereas the heterozygous SN allele seems to protect against the disease (*50*).

Only one study has been reported with armadillos and this described a non-synonymous polymorphism in TLR1 (A1879G – R627G) not reported in humans. A total of 6% of animals screened (all resistant to the disease) showed that homozygous G/G allele is associated with resistance to the disease (*28*).

The *TLR1* coding sequence of the 58 squirrel samples (54 red, 4 grey) was covered at least 100X (average coverage was 25,000X). Nucleotide sequences are available on NCBI (KX388139, KX388140 and KX388141). A multiple sequence alignment of the TLR1 protein sequence from red squirrel, grey squirrel, human and armadillo is given in Table S13. No polymorphisms were observed at sites associated with leprosy in humans and armadillos, neither in red nor in grey squirrels (Figure 3C, Table S13). However, polymorphisms were observed at A1478G (S493N), and a cluster of 8 nearby SNP producing S656N, L659V and N661C. Comparison of

infected red squirrels, regardless of the causative agent, (n=16) with healthy red squirrels (n=39) showed that the presence of alleles 493N and 656N-659V-661C was associated with resistance to leprosy (OR: 5.77, 95% CI: 1.42 – 23.41, *p*=0.01 for 494N and OR: 4.89, 95% CI: 0.98 – 24.53, *p*=0.05 for 657N-660V-662C).

A previous study in human has predicted a polymorphism in V651A to be potentially detrimental for signal activation (*51*). This valine is at the position 654 in *S. vulgaris*, only two amino acids before the first cluster of modifications. Therefore, the association of these polymorphisms with leprosy should be validated in a larger cohort.

In this study, we have compared the TLR1 sequences of 16 infected red squirrels with 42 non-infected red and grey squirrels. We found no significant difference within the *M. leprae* cohort (not applicable) and *M. lepromatosis* cohort (OR: 0.82, 95% CI: 0.12 – 5.51, *p*=0.84 for 494N and OR: 0.98, 95% CI: 0.15 – 6.57, *p*= 0.98 for 657N-660V-662C) when comparing infected to healthy specimens. However, taken together, we found a correlation between SNP and susceptibility to the disease. The SNP found have never been described in human and armadillos but occur in the LRR and TIR domains, thus they might have an impact on TLR recognition or function.

The extracellular domain of red squirrel TLR1 has 20 leucine-rich repeats (LRR). The mutation S493N is localized in the 19th (LRR) in the extracellular domain whereas the human mutation N251S is located in the 9th LRR. Both mutations are exposed to the solvent, on the same face of the ring (Fig. 4B), the glycan binding site situated on the opposite face of the ascending side, which is the dimerization interface (*47*), and both are localized in loop just in front of beta sheets. The human L607 seems to be in the membrane really close to the extracytoplasmic part while the R627 mutation in armadillos is located in the cytoplasmic domain. The patch of mutations affecting amino acids 656, 659, 661 is localized intracellularly and precisely in helix 1 of the TIR domain.

Supplementary tables and figures

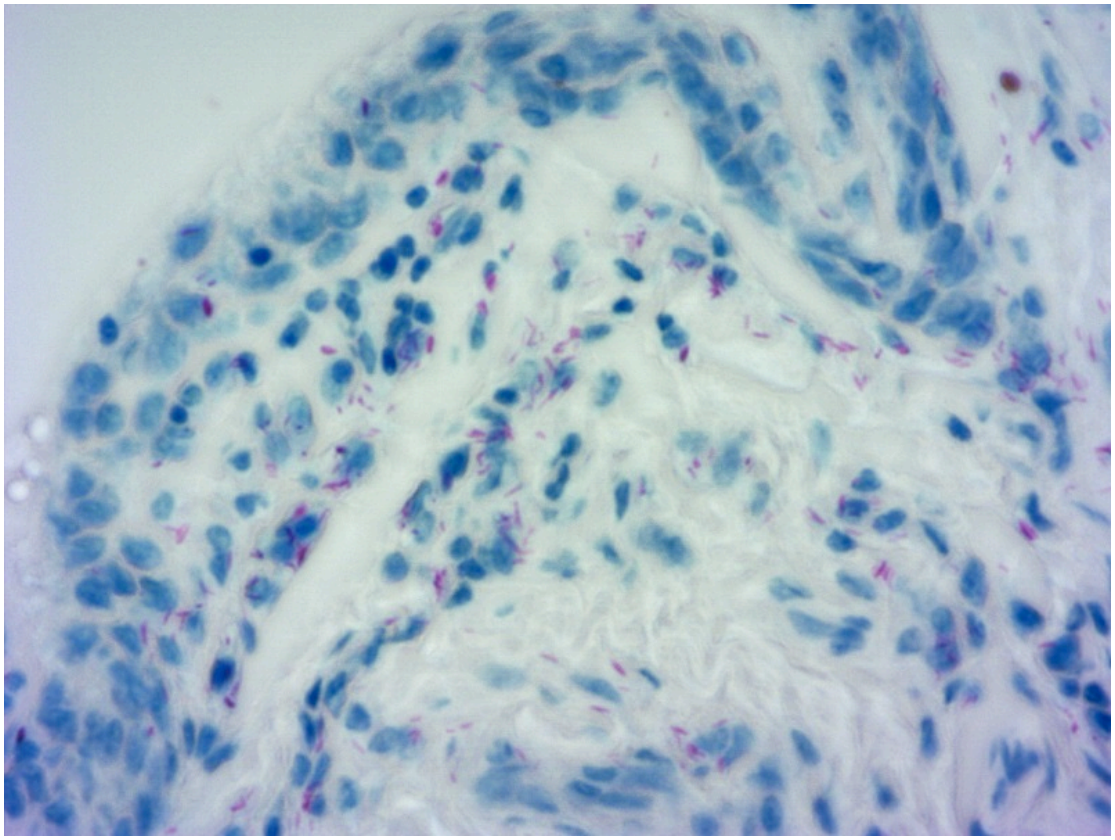

Figure S1: Numerous intra- and extracellular acid-fast bacilli in the footpad of a *M. lepromatosis* PCR+ red squirrel (Ir36). Ziehl-Neelsen stain x 600.

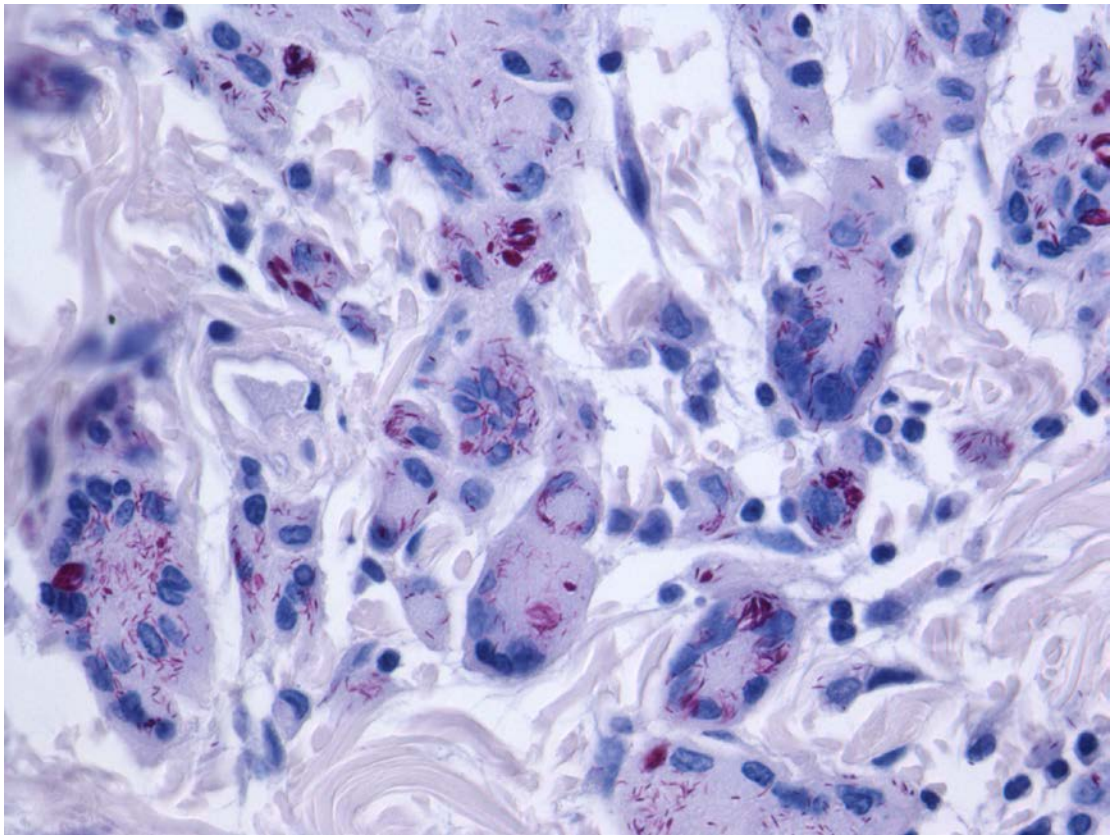

Figure S2: Giant cell formation and intracellular acid-fast bacilli in *M. lepromatosis* infected squirrel (mainly BL form in the section). ZN staining x 400.

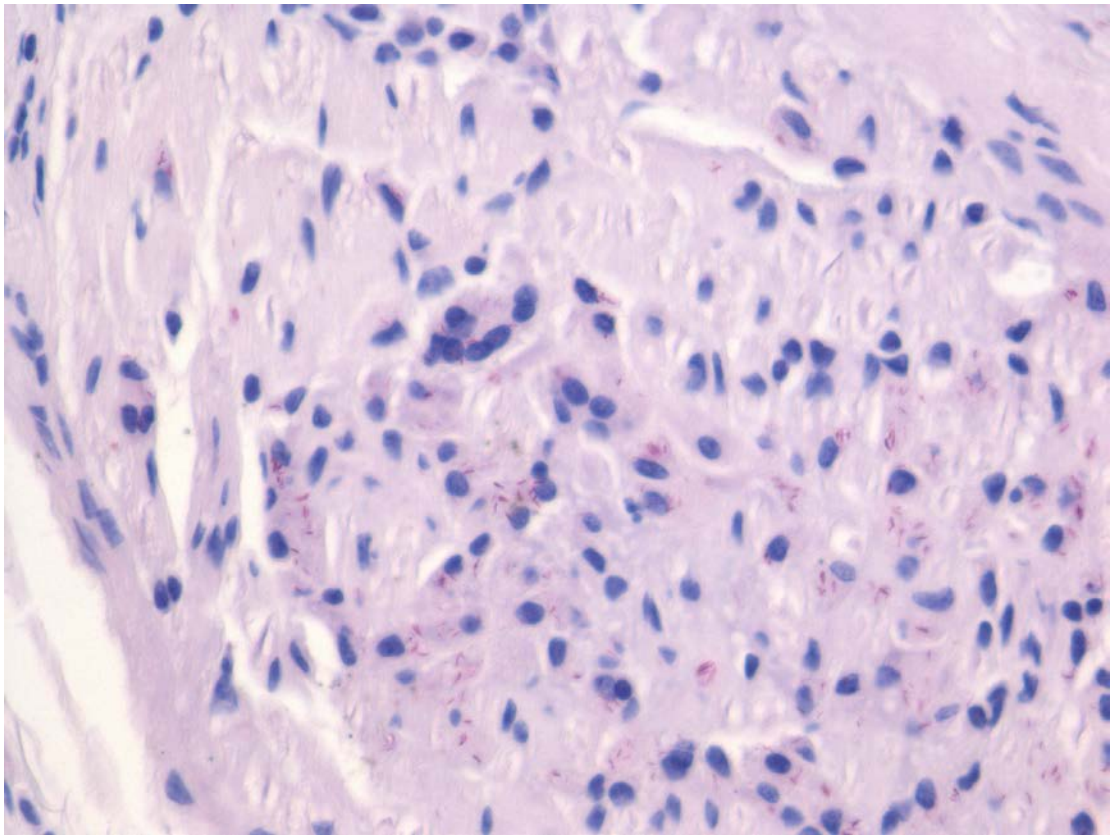

Figure S3: Borderline tuberculoid (BT) leprosy with intracellular acid-fast bacilli in the muzzle of a *M. leprae* PCR+ squirrel. ZN staining x 400.

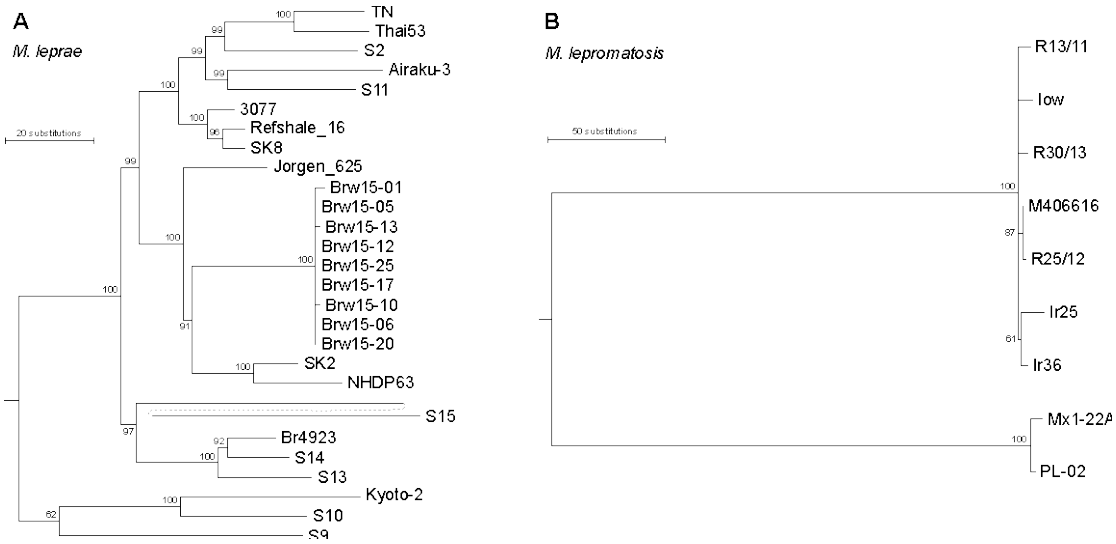

Figure S4: Phylogeny of *M. leprae* and *M. lepromatosis*. (A) Maximum Parsimony phylogenetic tree of *M. leprae* strains inferred from 671 genome-wide variable positions. Bootstrap support (from 500 replicates) is given for each node. *M. lepromatosis* was used as outgroup to root the tree. **(B)** Maximum Parsimony phylogenetic tree of *M. lepromatosis* strains inferred from 435 genome-wide variable positions. Bootstrap support (from 500 replicates) is given for each node. *M. leprae* was used as outgroup to root the tree.

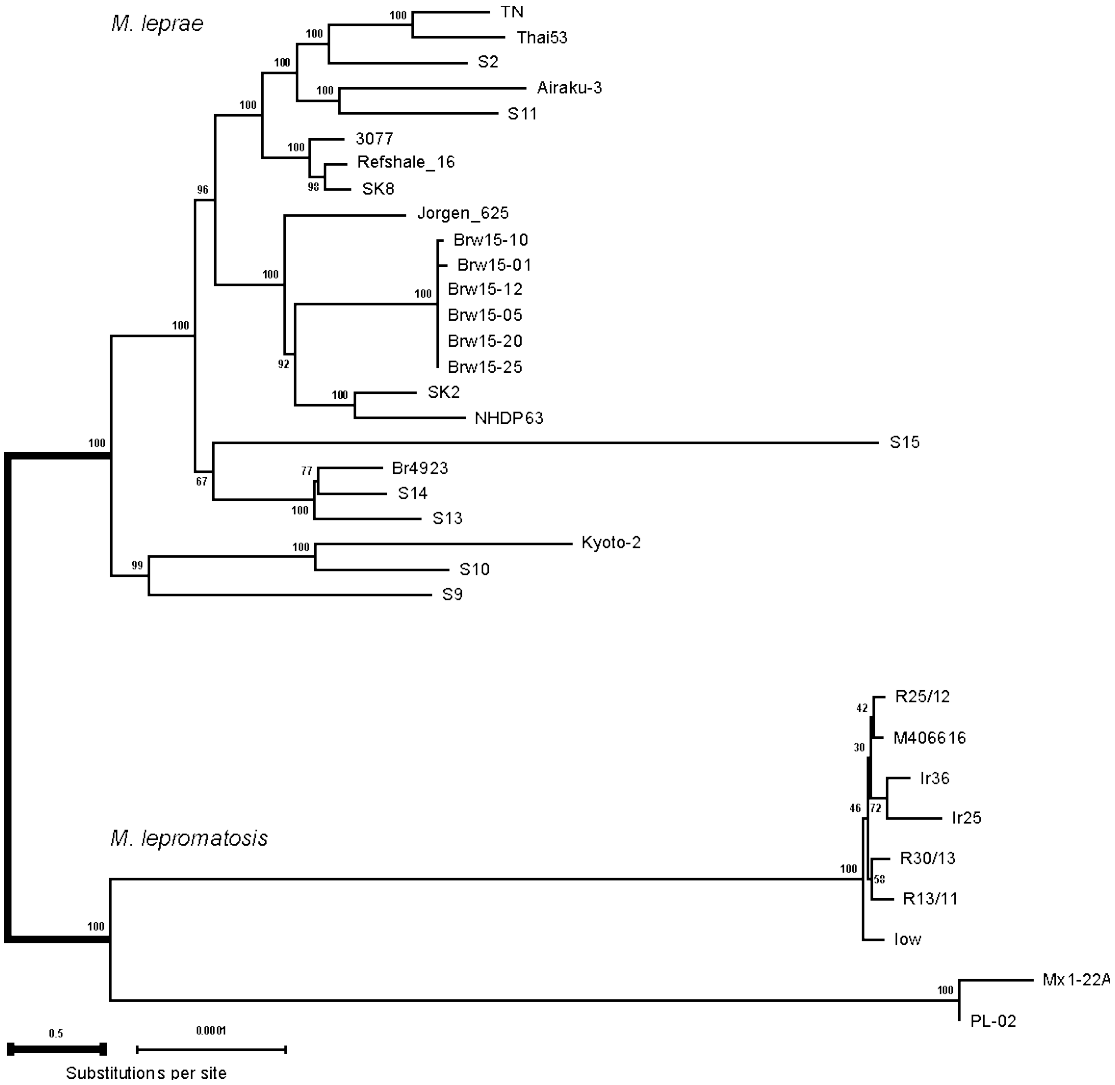

Fig S5: Phylogeny of *M. leprae* and *M. lepromatosis*. Neighbor-Joining phylogenetic tree of *M. leprae* and *M. lepromatosis* strains inferred from 307,159 genome-wide variable positions. Distances were computed using the p-distance method. Bootstrap support (from 500 replicates) is given for each node. The tree is drawn to scale. Note that the node dividing the two species (thick lines) was dramatically flattened to reduce space.

Table S1: Details of all specimens analyzed in this study from squirrels and human. NA: not available.

Table S2: Description of gross post-mortem examination in squirrels from Scotland and England. 1: presence of lesion 0: absence of lesion.

Table S3: PCR screening performed at EPFL and Moredun Institute. Pos: PCR positive; Neg: PCR negative; nt: not tested.

Table S4: Overview of the serology results. Only those squirrels tested are recorded in this table – 0= negative; 1= positive between 5 and 10 min of incubation, 2: positive before 5 min of incubation.

Table S5: Overview of the histopathological results obtained for red squirrels samples. 1: presence; 0: absence; NA: data not available; AFB= acid fast bacilli.

Table S6: List of samples and DNA extraction methods used in this study. NA: not available; 1: DNA extracted; 0: DNA not extracted.

Table S7: Summary of all the *M. leprae* and *M. lepromatosis* strains that were sequenced genome-wide in this study. Samples used in downstream analyses are in bold. E= ear, M= muzzle, L= liver, S= spleen, T= tail, H= hindlimb.

Table S8: Pairwise SNP difference between *M. lepromatosis* strains used in this study. Mx1-22A and Pl-02 derived from humans in Mexico while the rest derived from squirrels in the British Isles.

Table S9: Unique variants (in grey) to *M. leprae* from Brownsea Island squirrels compared to the reference genome (AL450380.1). Variants in lower case were below our coverage thresholds and were manually inferred from the alignments. The order of the samples is the following: Brw15-1E, Brw15-5E, Brw15-6M2, Brw15-10, Brw15-12M, Brw15-13L, Brw15-17L+M, Brw15-20M, Brw15-25E. NA: not available.

Table S10: Unique variants shared by all *M. leprae* 3I SNP subtype compared to other SNP types: Variants in lower case were below our coverage thresholds and were manually inferred from the alignments.

Table S11: Overview of geographical origin and infection status of the 58 squirrels for which TLR1 was analyzed.

Table S12: List of specimens for which long range PCR for TLR1 sequencing was done.

Table S13: Multiple sequence alignment of TLR1. Sites where association with leprosy was found are in bold.

Table S14: Primers used for targeting the red squirrel mitochondrial 12S ribosomal RNA gene and *TLR1*.

References

1. World Health Organization, Global leprosy: Update on the 2012 situation. *Wkly. Epidemiol. Rec.* **88**, 365–379 (2013). Medline

2. H. D. Donoghue, G. M. Taylor, A. Marcsik, E. Molnár, G. Pálfi, I. Pap, M. Teschler-Nicola, R. Pinhasi, Y. S. Erdal, P. Velemínsky, J. Likovsky, M. G. Belcastro, V. Mariotti, A. Riga, M. Rubini, P. Zaio, G. S. Besra, O. Y. Lee, H. H. Wu, D. E. Minnikin, I. D. Bull, J. O'Grady, M. Spigelman, A migration-driven model for the historical spread of leprosy in medieval Eastern and Central Europe. *Infect. Genet. Evol.* **31**, 250–256 (2015). Medline doi:10.1016/j.meegid.2015.02.001

3. V. J. Schuenemann, P. Singh, T. A. Mendum, B. Krause-Kyora, G. Jäger, K. I. Bos, A. Herbig, C. Economou, A. Benjak, P. Busso, A. Nebel, J. L. Boldsen, A. Kjellström, H. Wu, G. R. Stewart, G. M. Taylor, P. Bauer, O. Y. Lee, H. H. Wu, D. E. Minnikin, G. S. Besra, K. Tucker, S. Roffey, S. O. Sow, S. T. Cole, K. Nieselt, J. Krause, Genome-wide comparison of medieval and modern *Mycobacterium leprae*. *Science* **341**, 179–183 (2013). Medline doi:10.1126/science.1238286

4. A. Alter, A. Grant, L. Abel, A. Alcaïs, E. Schurr, Leprosy as a genetic disease. *Mamm. Genome* **22**, 19–31 (2011). Medline doi:10.1007/s00335-010-9287-1

5. S. H. Wong, S. Gochhait, D. Malhotra, F. H. Pettersson, Y. Y. Teo, C. C. Khor, A. Rautanen, S. J. Chapman, T. C. Mills, A. Srivastava, A. Rudko, M. B. Freidin, V. P. Puzyrev, S. Ali, S. Aggarwal, R. Chopra, B. S. Reddy, V. K. Garg, S. Roy, S. Meisner, S. K. Hazra, B. Saha, S. Floyd, B. J. Keating, C. Kim, B. P. Fairfax, J. C. Knight, P. C. Hill, R. A. Adegbola, H. Hakonarson, P. E. Fine, R. M. Pitchappan, R. N. Bamezai, A. V. Hill, F. O. Vannberg, Leprosy and the adaptation of human toll-like receptor 1. *PLOS Pathog.* **6**, e1000979 (2010). Medline doi:10.1371/journal.ppat.1000979

6. N. Fulton, L. F. Anderson, J. M. Watson, I. Abubakar, Leprosy in England and Wales 1953-2012: Surveillance and challenges in low incidence countries. *BMJ Open* **6**, e010608 (2016). Medline doi:10.1136/bmjopen-2015-010608

7. R. Sharma, P. Singh, W. J. Loughry, J. M. Lockhart, W. B. Inman, M. S. Duthie, M. T. Pena, L. A. Marcos, D. M. Scollard, S. T. Cole, R. W. Truman, Zoonotic leprosy in the southeastern United States. *Emerg. Infect. Dis.* **21**, 2127–2134 (2015). Medline doi:10.3201/eid2112.150501

8. R. Truman, Leprosy in wild armadillos. *Lepr. Rev.* **76**, 198–208 (2005). Medline

9. R. W. Truman, P. Singh, R. Sharma, P. Busso, J. Rougemont, A. Paniz-Mondolfi, A. Kapopoulou, S. Brisse, D. M. Scollard, T. P. Gillis, S. T. Cole, Probable zoonotic leprosy in the southern United States. *N. Engl. J. Med.* **364**, 1626–1633 (2011). Medline doi:10.1056/NEJMoa1010536

10. X. Y. Han, Y. H. Seo, K. C. Sizer, T. Schoberle, G. S. May, J. S. Spencer, W. Li, R. G. Nair, A new *Mycobacterium* species causing diffuse lepromatous leprosy. *Am. J. Clin. Pathol.* **130**, 856–864 (2008). Medline doi:10.1309/AJCPP72FJZZRRVMM

11. P. Singh, A. Benjak, V. J. Schuenemann, A. Herbig, C. Avanzi, P. Busso, K. Nieselt, J. Krause, L. Vera-Cabrera, S. T. Cole, Insight into the evolution and origin of leprosy bacilli from the genome sequence of *Mycobacterium lepromatosis*. *Proc. Natl. Acad. Sci. U.S.A.* **112**, 4459–4464 (2015). Medline doi:10.1073/pnas.1421504112

12. M. Carey, G. Hamilton, A. Poole, C. Lawton, *The Irish Squirrel Survey 2007* (COFORD, Dublin, 2007).

13. S. Harris, G. B. Corbet, *The Handbook of British Mammals* (Mammal Society/Blackwell Scientific, ed. 3, 1991).

14. D. M. Tompkins, A. W. Sainsbury, P. Nettleton, D. Buxton, J. Gurnell, Parapoxvirus causes a deleterious disease in red squirrels associated with UK population declines. *Proc. R. Soc. B* **269**, 529–533 (2002).

15. E. Stokstad, Red squirrels rising. *Science* **352**, 1268–1271 (2016). Medline doi:10.1126/science.352.6291.1268

16. Council of Europe, Convention on the Conservation of European Wildlife and Natural Habitats (ETS No. 104), Appendix III (1979); https://rm.coe.int/CoERMPublicCommonSearchServices/DisplayDCTMContent?documentId=0900001680304356.

17. A. Meredith, J. Del Pozo, S. Smith, E. Milne, K. Stevenson, J. McLuckie, Leprosy in red squirrels in Scotland. *Vet. Rec.* **175**, 285–286 (2014). Medline doi:10.1136/vr.g5680

18. V. Simpson, J. Hargreaves, H. Butler, T. Blackett, K. Stevenson, J. McLuckie, Leprosy in red squirrels on the Isle of Wight and Brownsea Island. *Vet. Rec.* **177**, 206–207 (2015). doi:10.1136/vr.h4491

19. See supplementary materials on *Science* Online.

20. J. S. Spencer, P. J. Brennan, The role of *Mycobacterium leprae* phenolic glycolipid I (PGL-I) in serodiagnosis and in the pathogenesis of leprosy. *Lepr. Rev.* **82**, 344–357 (2011). Medline

21. J. S. Velarde-Félix, G. Alvarado-Villa, L. Vera-Cabrera, “Lucio’s Phenomenon” Associated with *Mycobacterium lepromatosis*. *Am. J. Trop. Med. Hyg.* **94**, 483–484 (2016). Medline doi:10.4269/ajtmh.15-0439

22. L. Vera-Cabrera, W. Escalante-Fuentes, S. S. Ocampo-Garza, J. Ocampo-Candiani, C. A. Molina-Torres, C. Avanzi, A. Benjak, P. Busso, P. Singh, S. T. Cole, *Mycobacterium lepromatosis* infections in Nuevo León, Mexico. *J. Clin. Microbiol.* **53**, 1945–1946 (2015). Medline doi:10.1128/JCM.03667-14

23. M. Monot, N. Honoré, T. Garnier, N. Zidane, D. Sherafi, A. Paniz-Mondolfi, M. Matsuoka, G. M. Taylor, H. D. Donoghue, A. Bouwman, S. Mays, C. Watson, D. Lockwood, A. Khamesipour, Y. Dowlati, S. Jianping, T. H. Rea, L. Vera-Cabrera, M. M. Stefani, S. Banu, M. Macdonald, B. R. Sapkota, J. S. Spencer, J. Thomas, K. Harshman, P. Singh, P. Busso, A. Gattiker, J. Rougemont, P. J. Brennan, S. T. Cole, Comparative genomic and phylogeographic analysis of *Mycobacterium leprae*. *Nat. Genet.* **41**, 1282–1289 (2009). Medline doi:10.1038/ng.477

24. A. J. Drummond, A. Rambaut, BEAST: Bayesian evolutionary analysis by sampling trees. *BMC Evol. Biol.* **7**, 214 (2007). Medline doi:10.1186/1471-2148-7-214

25. B. P. Vieira, C. Fonseca, R. G. Rocha, Critical steps to ensure the successful reintroduction of the Eurasian red squirrel. *Anim. Biodivers. Conserv.* **38**, 49–58 (2015).

26. S. R. Krutzik, M. T. Ochoa, P. A. Sieling, S. Uematsu, Y. W. Ng, A. Legaspi, P. T. Liu, S. T. Cole, P. J. Godowski, Y. Maeda, E. N. Sarno, M. V. Norgard, P. J. Brennan, S. Akira, T. H. Rea, R. L. Modlin, Activation and regulation of Toll-like receptors 2 and 1 in human leprosy. *Nat. Med.* **9**, 525–532 (2003). Medline doi:10.1038/nm864

27. C. de Sales Marques, V. N. Brito-de-Souza, L. T. Guerreiro, J. H. Martins, E. P. Amaral, C. C. Cardoso, I. M. Dias-Batista, W. L. Silva, J. A. Nery, P. Medeiros, P. Gigliotti, A. P. Campanelli, M. Virmond, E. N. Sarno, M. T. Mira, F. C. Lana, E. R. Caffarena, A. G. Pacheco, A. C. Pereira, M. O. Moraes, Toll-like receptor 1 N248S single-nucleotide polymorphism is associated with leprosy risk and regulates immune activation during mycobacterial infection. *J. Infect. Dis.* **208**, 120–129 (2013). Medline doi:10.1093/infdis/jit133

28. L. B. Adams, M. T. Pena, R. Sharma, D. A. Hagge, E. Schurr, R. W. Truman, Insights from animal models on the immunogenetics of leprosy: A review. *Mem. Inst. Oswaldo Cruz* **107** (suppl. 1), 197–208 (2012). Medline doi:10.1590/S0074-02762012000900028

29. P. G. Jessamine, M. Desjardins, T. Gillis, D. Scollard, F. Jamieson, G. Broukhanski, P. Chedore, A. McCarthy, Leprosy-like illness in a patient with *Mycobacterium lepromatosis* from Ontario, Canada. *J. Drugs Dermatol.* **11**, 229–233 (2012). Medline

30. P. Lurz, *Red Squirrel: Naturally Scottish* (Scottish Natural Heritage, 2010).

31. V. R. Simpson, J. Hargreaves, H. M. Butler, N. J. Davison, D. J. Everest, Causes of mortality and pathological lesions observed post-mortem in red squirrels (*Sciurus vulgaris*) in Great Britain. *BMC Vet. Res.* **9**, 229 (2013). Medline doi:10.1186/1746-6148-9-229

32. D. S. Ridley, W. H. Jopling, Classification of leprosy according to immunity. A five-group system. *Int. J. Lepr. Mycobact. Dis.* **34**, 255–273 (1966). Medline

33. A. M. Phillippy, X. Deng, W. Zhang, S. L. Salzberg, Efficient oligonucleotide probe selection for pan-genomic tiling arrays. *BMC Bioinformatics* **10**, 293 (2009). Medline doi:10.1186/1471-2105-10-293

34. A. M. Bolger, M. Lohse, B. Usadel, Trimmomatic: A flexible trimmer for Illumina sequence data. *Bioinformatics* **30**, 2114–2120 (2014). Medline doi:10.1093/bioinformatics/btu170

35. B. Langmead, S. L. Salzberg, Fast gapped-read alignment with Bowtie 2. *Nat. Methods* **9**, 357–359 (2012). Medline doi:10.1038/nmeth.1923

36. S. M. Kiełbasa, R. Wan, K. Sato, P. Horton, M. C. Frith, Adaptive seeds tame genomic sequence comparison. *Genome Res.* **21**, 487–493 (2011). Medline doi:10.1101/gr.113985.110

37. D. C. Koboldt, Q. Zhang, D. E. Larson, D. Shen, M. D. McLellan, L. Lin, C. A. Miller, E. R. Mardis, L. Ding, R. K. Wilson, VarScan 2: Somatic mutation and copy number alteration discovery in cancer by exome sequencing. *Genome Res.* **22**, 568–576 (2012). Medline doi:10.1101/gr.129684.111

38. K. Tamura, G. Stecher, D. Peterson, A. Filipski, S. Kumar, MEGA6: Molecular Evolutionary Genetics Analysis version 6.0. *Mol. Biol. Evol.* **30**, 2725–2729 (2013). Medline doi:10.1093/molbev/mst197

39. M. Nei, S. Kumar, *Molecular Evolution and Phylogenetics* (Oxford Univ. Press, 2000).

40. C. M. Johnson, E. A. Lyle, K. O. Omueti, V. A. Stepensky, O. Yegin, E. Alpsoy, L. Hamann, R. R. Schumann, R. I. Tapping, Cutting edge: A common polymorphism impairs cell surface trafficking and functional responses of TLR1 but protects against leprosy. *J. Immunol.* **178**, 7520–7524 (2007). Medline doi:10.4049/jimmunol.178.12.7520

41. *Practical Statistics for Medical Research* (CRC Press, 1990); www.crcpress.com/Practical-Statistics-for-Medical-Research/Altman/p/book/9780412276309.

42. L. A. Kelley, S. Mezulis, C. M. Yates, M. N. Wass, M. J. E. Sternberg, The Phyre2 web portal for protein modeling, prediction and analysis. *Nat. Protoc.* **10**, 845–858 (2015). Medline doi:10.1038/nprot.2015.053

43. M. Biasini, S. Bienert, A. Waterhouse, K. Arnold, G. Studer, T. Schmidt, F. Kiefer, T. Gallo Cassarino, M. Bertoni, L. Bordoli, T. Schwede, SWISS-MODEL: Modelling protein tertiary and quaternary structure using evolutionary information. *Nucleic Acids Res.* **42**, W252–W258 (2014). Medline doi:10.1093/nar/gku340

44. M. S. Jin, S. E. Kim, J. Y. Heo, M. E. Lee, H. M. Kim, S. G. Paik, H. Lee, J. O. Lee, Crystal structure of the TLR1-TLR2 heterodimer induced by binding of a tri-acylated lipopeptide. *Cell* **130**, 1071–1082 (2007). Medline doi:10.1016/j.cell.2007.09.008

45. Y. Xu, X. Tao, B. Shen, T. Horng, R. Medzhitov, J. L. Manley, L. Tong, Structural basis for signal transduction by the Toll/interleukin-1 receptor domains. *Nature* **408**, 111–115 (2000). doi:10.1038/35040600

46. K. Zhou, R. Kanai, P. Lee, H.-W. Wang, Y. Modis, Toll-like receptor 5 forms asymmetric dimers in the absence of flagellin. *J. Struct. Biol.* **177**, 402–409 (2012). Medline doi:10.1016/j.jsb.2011.12.002

47. I. Botos, D. M. Segal, D. R. Davies, The structural biology of Toll-like receptors. *Structure* **19**, 447–459 (2011). Medline doi:10.1016/j.str.2011.02.004

48. A. Krogh, B. Larsson, G. von Heijne, E. L. Sonnhammer, Predicting transmembrane protein topology with a hidden Markov model: Application to complete genomes. *J. Mol. Biol.* **305**, 567–580 (2001). Medline doi:10.1006/jmbi.2000.4315

49. L. L. C. Schrödinger, The PyMOL molecular graphics system, version 1.8 (2015).

50. R. P. Schuring, L. Hamann, W. R. Faber, D. Pahan, J. H. Richardus, R. R. Schumann, L. Oskam, Polymorphism N248S in the human Toll-like receptor 1 gene is related to leprosy and leprosy reactions. *J. Infect. Dis.* **199**, 1816–1819 (2009). Medline doi:10.1086/599121

51. M. Ben-Ali, B. Corre, J. Manry, L. B. Barreiro, H. Quach, M. Boniotto, S. Pellegrini, L. Quintana-Murci, Functional characterization of naturally occurring genetic variants in the human TLR1-2-6 gene family. *Hum. Mutat.* **32**, 643–652 (2011). Medline doi:10.1002/humu.21486